J Fluoresc (2015) 25:1517–1526
DOI 10.1007/s10895-015-1643-9

ORIGINAL ARTICLE

Fluorescent Properties of 8-Substituted BODIPY Dyes: Influence of Solvent Effects

Yuriy S. Marfin[1] · **Dmitry A. Merkushev**[1] · **Sergey D. Usoltsev**[1] · **Maria V. Shipalova**[1] · **Evgeniy V. Rumyantsev**[1]

Received: 27 May 2015 / Accepted: 6 August 2015 / Published online: 18 August 2015

Abstract Three boron-dipyrrine (BODIPY) based dyes with bulky substituents in 8-position of dipyrrin ligand have been synthesized and characterized. Photophysical properties of the obtained compounds have been investigated in different individual solvents and solvent mixtures. Investigated compounds was found to be intensive fluorescent molecular rotors. The influence of different solvent parameters and the substituent nature on rotor characteristics have been observed and discussed. Minor changes in the nature of 8-substituent does not influence the spectral properties, but the presence of nitrogen donor atom in the phenyl substituent could be used for the sensing of the donor-acceptor interactions with solvent or dissolved compounds. The new approach of spectral properties correlation with solvent parameters was proposed, the viscosity parameter should be taken into account in case of BODIPYs with bulky substituents. The intensity of fluorescence molecular rotor properties decrease gradually with the viscosity increase above 1 cP.

Keywords Fluorescent molecular rotors · BODIPY · Dynamic viscosity · Photophysical properties · Solvent parameters

Introduction

An increased interest for fluorescent small molecules has inspired the development of a large variety of fluorescence-based spectroscopic and imaging techniques. Nowadays, boron-dipyrrine (BODIPY, 4,4-difluoro-4-bora-3a,4a-diaza-s-indacene) based compounds are one of the most commonly used fluorescent sensors and labels, due to high photostability and fluorescence quantum yields. BODIPY-based fluorescent sensors may be used for selective detection of cations [1, 2], anions [3, 4] and measurement of pH [5, 6]. These sensors also serve effectively the purposes of biochemistry and molecular biology [7–9]. Another approach of sensors is covalent bonding of BODIPY luminophores to various biomolecules for further usage [10].

The newest direction in BODIPY-based dyes properties studies is obtainment of new fluorescent molecular rotors [11, 12]. While being exited one part of those molecules are able to rotate towards the other, causing the intramolecular charge transfer (this effect is called twisted intramolecular charge transfer state, or TICT state) [13, 14]. The main feature of such molecular rotors is a strong dependence between its quantum yield and solvent dynamic viscosity. In this case, low viscosity mixtures may cause low relative fluorescence quantum yields due to high probability of non-radiative transition [15]. Fluorescent molecular sensors gain much popularity in molecular biology, analytical and biochemical studies nowadays [16]. It is caused by extremely high value of analytical feedback and high compound and properties selectivity. In this case quantum yield φ and solvent bulk viscosity η follow a power-law relationship that is widely referred to as the Forster-Hoffmann equation [17]: $\log\varphi = x \cdot \log\eta + C$, where C and x are solvent- and dye-dependent constants. This relationship has been experimentally shown to be valid in a wide range of viscosities and in both polar and nonpolar fluids.

Despite the large number of publications, no attempts of systematic investigations of solvent influence on the BODIPY-based fluorescent molecular rotors with bulky substituents were made. Considering these facts, we tried to

✉ Yuriy S. Marfin
ymarfin@gmail.com

[1] Department of Inorganic Chemistry, Ivanovo State University of Chemistry and Technology, 7 Sheremetevsky str, 153000 Ivanovo, Russia

understand the role of different solvent parameters on BODIPY spectral properties in terms of solvatochromic approach.

Experimental

Synthesis

Complexes of BODIPY, differing by the nature of the substituent in the 8- position of the dipyrrin ligand, were synthesized and investigated. 4,4-difluoro-8-phenyl-1,3,5,7-tetramethyl-2,6-diethyl-4-boron-3a,4a-diaza-s-indacene (***1***), 4,4-difluoro-8-(4-dimethylaminephenyl)-1,3,5,7-tetramethyl-2,6-diethyl-4-boron-3a,4a-diaza-s-indacene (***2***), 4,4-difluoro-8-(3,5-dimethylphenyl)-1,3,5,7-tetramethyl-2,6-diethyl-4-boron-3a,4a-diaza-s-indacene (***3***) were synthesized by the methods described above. The reagents were obtained from Sigma-Aldrich and were readily used in the synthetic procedures.

Common Synthesis of 8-Substituted BODIPY

An appropriate aldehyde (0.002 mol) and 2,4-dimethyl-3-ethylpyrrole (0.004 mol) were dissolved in 50 ml of absolute dichloromethane (CH_2Cl_2). One drop of trifluoroacetic acid (CF_3COOH) was added, and the solution was steered for 12 h at room temperature. Then 0.002 mol of 2,3-dichloro-5,6-dicyano-1,4-benzoquinone (DDQ) was added and the solution was stirred for 20 min. The excess of boron trifluoride diethyl etherate ($BF_3O(Et)_2$, 4 ml) and triethylamine ($N(Et)_3$, 4 ml) was added and stirring was continued for 30 min (Fig. 1). The intense fluorescence of reaction mixture was observed on that stage. The formation of intermediates and BODIPY products on every stage were controlled by changes in electron absorption spectra of the solution. After synthesis the reaction mixture was washed with water, dried over anhydrous $MgSO_4$, filtered and evaporated. The resulting product was purified by silica gel chromatography (eluent – $C_2H_2Cl_2$/hexane) to afford analytically pure samples.

Conducting the one pot synthesis allowed us to reduce losses associated with the isolation and purification of intermediates and to increase the yields of target BODIPY.

4,4-difluoro-8-phenyl-1,3,5,7-tetramethyl-2,6-diethyl-4-boron-3a,4a-diaza-s-indacene was synthesized according to the general synthesis procedure using benzaldehyde as a precursor. The reaction product is dark red crystals (yield=75 %). ^{1}H NMR (500 MHz, CCl_4): δ 1.1(T,6H), 2.25(S,6H), 2.45(D, 4H), 2.73(S,6H), 7.16(S,5H). MALDI-TOF: calculated ($[C_{23}H_{27}BF_2N_2]^+$) *m*/*z*=377.26, found *m*/*z*=377.99. Anal. Calculated for: $C_{23}H_{27}BF_2N_2$: C, 83.34; H, 8.21; N, 8.45. Found: C, 83.23; H, 8.27; N, 8.53.

4,4-difluoro-8-(4-dimethylaminephenyl)-1,3,5,7-tetramethyl-2,6-diethyl-4-boron-3a,4a-diaza-s-indacene was synthesized according to the general synthesis procedure using 4-dimethylaminobenzaldehyde as a precursor. The reaction product is dark green crystals (yield=64 %). ^{1}H NMR(500 MHz, CCl_4): δ 1.5(Q,6H), 2.53 (D,4H), 3.07(S, 6H), 3.12(S,6H), 3,38(S,6H), 6.85(D, 2H), 7.08(D,2H).

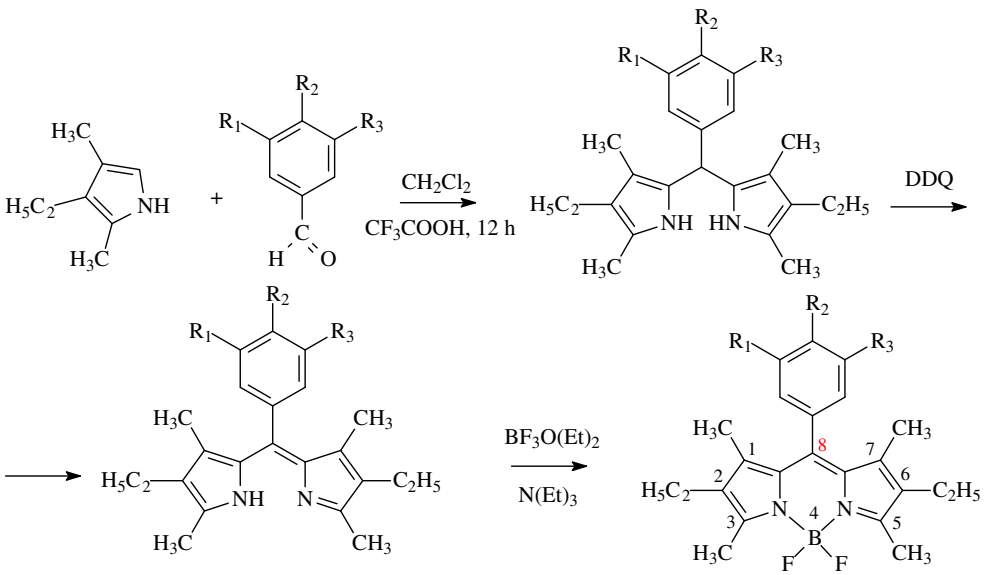

Fig. 1 Synthetic route to BODIPY dyes

R_1 = H, R_2 = H, R_3 = H;
R_1 = H, R_2 = $N(CH_3)_2$, R_3 = H;
R_1 = CH_3, R_2 = H, R_3 = CH_3

Table 1 The change of rheological characteristics of the solvents under the temperature variations [35]

T, K	*η*, cP			
	CCl_4	C_6H_6	C_6H_{12}	C_2H_5OH
293	0.969	0.652	0.307	1.200
298	0.900	0.600	0.294	1.096
303	0.843	0.559	0.29	1.003
308	0.791	0.531	0.272	0.919
313	0.739	0.503	0.253	0.834
318	0.695	0.470	0.251	0.768
323	0.651	0.436	0.248	0.702
328	0.618	0.413	0.235	0.647
333	0.585	0.389	0.222	0.592
338	0.560	0.374	0.219	0.529
343	0.534	0.357	0.216	0.483

MALDI-TOF: calculated ($[C_{25}H_{32}BF_2N_3]^+$) *m*/*z*=420.33, found *m*/*z*=420.96. Anal. Calculated for: $C_{25}H_{32}BF_2N_3$: C, 80.17; H, 8.61; N, 11.22. Found: C, 80.14; H, 8.63; N, 11.30.

4,4-difluoro-8-(3,5-dimethylphenyl)-1,3,5,7-tetramethyl-2,6-diethyl-4-boron-3a,4a-diaza-s-indacene was synthesized according to the general synthesis procedure using 3,5-dimethylbenzaldehyde as a precursor. The reaction product is dark green crystals (yield=68 %). ^{1}H NMR(500 MHz, CCl_4): δ 1.1(T,6H), 2.25(S,6H), 2.45(D,4H), 2.73(S,6H), 6.93(S,2H), 7.03(S,1H). MALDI-TOF: calculated ($[C_{25}H_{31}BF_2N_2]^+$) *m*/*z*=405.31, found *m*/*z*=405.86. Anal. Calculated for: $C_{25}H_{31}BF_2N_2$: C, 83.52; H, 8.69; N, 7.79. Found: C, 83.52; H, 8.70; N, 7.79.

Organic Solvents

The measurements were held in individual organic solvents of different nature and their mixtures. Solvents (Chimmed, Russia) were all of analytical grade purified by standard techniques [18]. The residual water content (<0.02 %) was determined by the Karl Fischer method [19]. The changing of the viscosity was achieved by varying the solution temperature in range 293 to 343 K (Table 1), and by varying the components molar ratios in mixtures of 2-propanol (low viscosity solvent) and glycerol (high viscosity solvent) to change the viscosity of the dyes' solution in a broad range 11.5–1444 cP.

NMR spectra were recorded on AVANCE500 (Bruker) at 500 MHz for ^{1}H NMR. Mass spectra (MS) were measured with AXIMA Confidence (Shimadzu) MALDI-TOF mass spectrometer.

UV–Vis electronic absorption spectra (EAS) were recorded in the range 350–800 nm on an SF-104 spectrophotometer (Aquilon, Russia) controlled with a PC through the software package UVWin 5.1.0. The accuracy of the measurements was±0.03 on the scale of optical density; wavelength accuracy was±0.05 nm. The fluorescence spectra were obtained with a Cary Eclipse fluorescence spectrometer (Varian-Agilent, US-Australia) controlled with a PC using the software package Cary Eclipse Scan Application 1.1. The fluorescence spectra were measured in the wavelength range 500–900 nm and the excitation wavelength was 480 nm. The slit widths of excitation and emission ranged from 2.5 to 5 nm. Investigations were carried out in quartz cuvettes with a thickness of the absorbing layer of 2 and 10 mm. All experiments were performed in a temperature-controlled cell with Peltier PTC-2 module at fixed temperatures of 283 to 343 K.

Fluorescence quantum yield (*φ*) was defined as follows:

$$\varphi_x = \varphi_{st} \cdot \left(\frac{A_x}{A_{st}}\right) \cdot \left(\frac{B_{st}}{B_x}\right) \cdot \left(\frac{\eta_x^2}{\eta_{st}^2}\right)$$

where φ_{st} is the rhodamine 6G standard quantum yield in ethanol (φ=0.95, [20]), A_x and A_{st} are the integrated area under the corrected fluorescence spectra, B_x and B_{st} are the absorbance (optical density) at the excitation wavelength, n_x and n_{st} are the refractive indices of solvents used for two solutions.

Nonradiative (k_{nr}) and radiative decay constants (k_{fl}) were calculated from experimentally measured fluorescence quantum yield *φ* and calculated fluorescence lifetime *τ* according to the following equations:

$$\varphi = \frac{k_{fl}}{k_{fl} + k_{nr}}; \rightarrow\rightarrow \tau = \frac{1}{k_{fl} + k_{nr}}$$

Result and Discussion

Photophysical Characteristics

Electronic absorption spectra of investigated complexes are characterized by intensive absorption maxima between 522

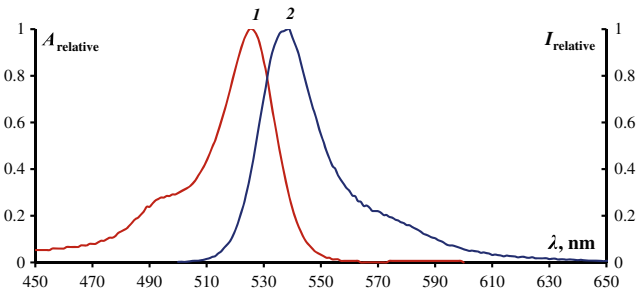

Fig. 2 Electronic absorption spectrum (*1*) and fluorescence spectrum (*2*) of complex **2** in benzene

Table 2 Photophysical characteristics of investigated compounds

	λ_{abs}, nm	λ_{fl}, nm	φ^{293}	τ^{293}, ns	$k^{293}_{rad}\cdot 10^8$	$k^{293}_{nrad}\cdot 10^8$	*X*	*C*
CCl_4								
1	527	539	0.778	1.60	0.49	5.76	0.838	−0.078
2	526	538	0.795	1.06	0.75	8.65	0.771	−0.089
3	526	540	0.904	0.83	1.08	10.90	0.397	−0.025
C_6H_6								
1	527	541	0.713	1.35	0.53	6.87	0.595	−0.021
2	526	540	0.741	0.85	0.87	10.91	0.771	0.023
3	526	540	0.961	0.92	1.04	9.80	0.547	0.092
C_6H_{12}								
1	524	536	0.938	1.80	5.03	0.52	1.153	0.576
2	531	537	0.923	1.24	7.31	0.74	0.445	0.197
3	523	536	0.951	0.89	1.06	10.10	1.138	0.576
C_2H_5OH								
1	522	534	0.768	1.35	0.57	6.84	0.535	−0.113
2	526	537	0.583	0.57	1.02	16.40	0.052	−0.236
3	523	537	0.974	0.84	1.16	10.72	0.269	−0.027

λ_{abs} the wavelength of maximum absorption, λ_{fl} the wavelength of maximum fluorescence, φ fluorescence quantum yield at 293 K, τ excited state lifetime at 293 K, k^{293}_{rad} radiative deactivation rate constant at 293 K, k^{293}_{nrad} non-radiative deactivation rate constant at 293 K and the Forster-Hoffman equation constants (*X*, *C*)

and 531 nm corresponding to an electronic transition $S_0 - S_1$. Fluorescence peaks are between 534 and 541 nm (Fig. 2).

The nature of the substituent in the 8-position doesn't have much influence on the fluorescence and absorption maxima positions (Table 2). The transition from non-polar solvents to polar ethanol is accompanied by the hypsochromic shift for all investigated compounds. The average Stokes shifts of fluorescence (12 – 14 nm) for investigated molecules are higher than the shift of BODIPY compounds with H- substituents in 8-position and approximately equal to commercial CH_3-substituted analogies [21, 22]. It is associated with the increase of the ability to dissipate energy by rotational and vibrational relaxation. The highest values of relative fluorescence quantum yields were observed for compound ***3***. The difference between quantum yields of **1** and **2** is minor for all solvents except ethanol. Excited state lifetimes of the investigated molecules lie between 0.83 and 1.80 ns, which is in agreement with published data for similar complexes [23]. Compound ***1*** has the highest excited state lifetime. The non-radiative deactivation constants are an order of magnitude higher than the radiative ones that confirms the assumption of non-radiative deactivation ability by the TICT state formation.

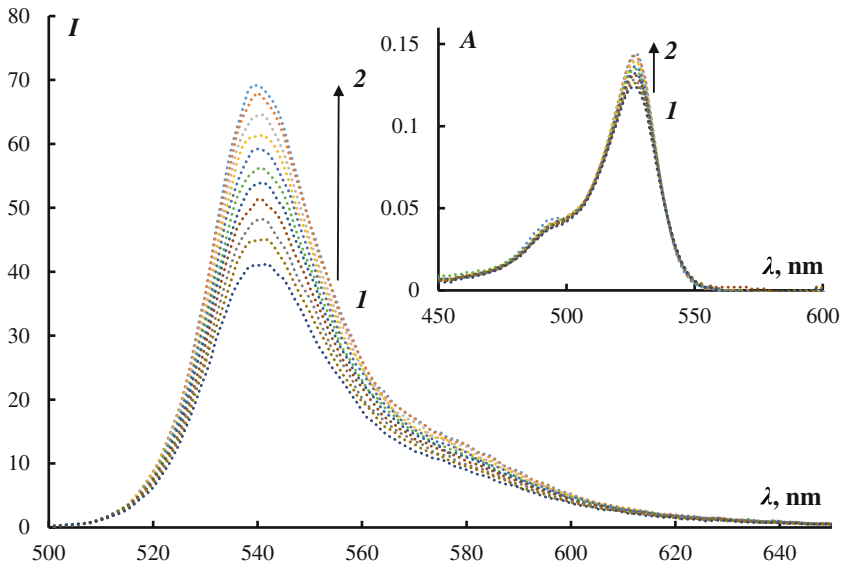

Fig. 3 Fluorescence spectra and absorption spectra (incut) of compound *1* in CCl_4 with different viscosities: *1* – 0.534 cP, *2* – 0.969 cP

Table 3 The change of photophysical characteristics of tested compounds in dependence on the viscosity of different solvents

1											
	CCl_4										
η, cP	0.969	0.900	0.843	0.791	0.739	0.695	0.651	0.618	0.585	0.561	0.534
φ	0.778	0.759	0.724	0.697	0.667	0.633	0.607	0.573	0.536	0.505	0.465
τ, ns	1.60	1.56	1.49	1.43	1.38	1.31	1.26	1.19	1.12	1.06	0.99
$k_{rad}\cdot 10^8$	0.49	0.49	0.49	0.49	0.49	0.48	0.48	0.48	0.48	0.48	0.47
$k_{nrad}\cdot 10^8$	5.76	5.91	6.22	6.48	6.78	7.16	7.47	7.91	8.44	8.92	9.66
	C_6H_6										
η, cP	0.652	0.600	0.559	0.531	0.503	0.4695	0.436	0.4125	0.389	0.374	0.357
φ	0.713	0.686	0.694	0.668	0.636	0.611	0.602	0.566	0.557	0.522	0.491
τ, ns	1.35	1.29	1.31	1.26	1.20	1.16	1.14	1.08	1.07	1.01	0.96
$k_{rad}\cdot 10^8$	0.53	0.53	0.53	0.53	0.53	0.53	0.53	0.52	0.52	0.52	0.51
$k_{nrad}\cdot 10^8$	6.87	7.17	7.09	7.39	7.78	8.11	8.21	8.72	8.83	9.38	9.93
	C_6H_{12}										
η, cP	0.307	0.294	0.290	0.272	0.253	0.251	0.248	0.235	0.222	0.219	0.216
φ	0.938	0.921	0.898	0.863	0.877	0.789	0.745	0.705	0.723	0.808	0.631
τ, ns	1.80	1.49	1.46	1.40	1.43	1.30	1.23	1.17	1.21	1.37	1.08
$k_{rad}\cdot 10^8$	0.52	0.62	0.62	0.62	0.61	0.61	0.61	0.60	0.60	0.59	0.58
$k_{nrad}\cdot 10^8$	5.03	6.09	6.25	6.51	6.37	7.11	7.52	7.92	7.65	6.71	8.67
	C_2H_5OH										
η, cP	1.200	1.096	1.003	0.919	0.834	0.768	0.702	0.647	0.592	0.529	0.483
φ	0.768	0.805	0.769	0.735	0.701	0.671	0.645	0.612	0.578	0.550	0.517
τ, ns	1.35	1.42	1.36	1.30	1.24	1.19	1.15	1.10	1.04	1.00	0.94
$k_{rad}\cdot 10^8$	0.57	0.57	0.57	0.57	0.56	0.56	0.56	0.56	0.56	0.55	0.55
$k_{nrad}\cdot 10^8$	6.84	6.48	6.81	7.12	7.49	7.81	8.12	8.54	9.04	9.48	10.0
2											
	CCl_4										
η, cP	0.969	0.900	0.843	0.791	0.739	0.695	0.651	0.618	0.585	0.561	0.534
φ	0.795	0.729	0.728	0.686	0.643	0.635	0.583	0.556	0.534	0.516	0.506
τ, ns	1.06	0.97	0.97	0.92	0.86	0.85	0.79	0.75	0.73	0.71	0.70
$k_{rad}\cdot 10^8$	0.75	0.75	0.75	0.75	0.75	0.74	0.74	0.74	0.74	0.73	0.73
$k_{nrad}\cdot 10^8$	8.65	9.51	9.52	10.20	10.9	11.0	12.0	12.5	13.0	13.4	13.6
	C_6H_6										
η, cP	0.652	0.600	0.559	0.531	0.503	0.4695	0.436	0.4125	0.389	0.374	0.357
φ	0.741	0.712	0.682	0.655	0.618	0.583	0.564	0.552	0.520	0.488	0.458
τ, ns	0.85	0.82	0.78	0.75	0.71	0.67	0.65	0.64	0.60	0.57	0.54
$k_{rad}\cdot 10^8$	0.87	0.87	0.87	0.87	0.87	0.87	0.87	0.87	0.86	0.86	0.85
$k_{nrad}\cdot 10^8$	10.9	11.4	11.9	12.5	13.3	14.1	14.5	14.8	15.7	16.7	17.7
	C_6H_{12}										
η, cP	0.307	0.294	0.290	0.272	0.253	0.251	0.248	0.235	0.222	0.219	0.216
φ	0.923	0.911	0.917	0.883	0.864	0.856	0.839	0.831	0.811	0.800	0.789
τ, ns	1.24	1.20	1.21	1.17	1.15	1.15	1.13	1.13	1.11	1.11	1.10
$k_{rad}\cdot 10^8$	0.74	0.76	0.76	0.75	0.75	0.75	0.74	0.74	0.73	0.72	0.71
$k_{nrad}\cdot 10^8$	7.31	7.55	7.48	7.76	7.92	7.96	8.09	8.11	8.26	8.30	8.34
	C_2H_5OH										
η, cP	1.200	1.096	1.003	0.919	0.834	0.768	0.702	0.647	0.592	0.529	0.483
φ	0.583	0.581	0.583	0.583	0.575	0.573	0.571	0.567	0.567	0.560	0.558
τ, ns	0.57	0.57	0.57	0.58	0.57	0.57	0.57	0.57	0.57	0.57	0.57
$k_{rad}\cdot 10^8$	1.02	1.02	1.02	1.01	1.01	1.01	1.00	1.00	0.99	0.99	0.98
$k_{nrad}\cdot 10^8$	16.4	16.5	16.4	16.4	16.5	16.6	16.6	16.6	16.5	16.6	16.6

Table 3 (continued)

3											
	CCl_4										
η, cP	0.969	0.900	0.843	0.791	0.739	0.695	0.651	0.618	0.585	0.561	0.534
φ	0.904	0.899	0.890	0.867	0.850	0.838	0.815	0.792	0.764	0.738	0.712
τ, ns	0.83	0.83	0.82	0.80	0.79	0.78	0.76	0.74	0.72	0.70	0.68
$k_{rad}\cdot10^8$	1.08	1.08	1.09	1.08	1.08	1.08	1.08	1.07	1.07	1.06	1.05
$k_{nrad}\cdot10^8$	10.9	11.0	11.1	11.4	11.7	11.8	12.1	12.5	12.9	13.3	13.7
	C_6H_6										
η, cP	0.652	0.600	0.559	0.531	0.503	0.4695	0.436	0.4125	0.389	0.374	0.357
φ	0.961	0.925	0.902	0.880	0.857	0.829	0.805	0.767	0.740	0.716	0.684
τ, ns	0.92	0.89	0.86	0.84	0.82	0.80	0.77	0.74	0.72	0.70	0.68
$k_{rad}\cdot10^8$	1.04	1.04	1.04	1.05	1.04	1.04	1.04	1.03	1.03	1.02	1.01
$k_{nrad}\cdot10^8$	9.80	10.2	10.5	10.8	11.1	11.5	11.9	12.5	12.9	13.2	13.8
	C_6H_{12}										
η, cP	0.307	0.294	0.290	0.272	0.253	0.251	0.248	0.235	0.222	0.219	0.216
φ	0.951	0.928	0.897	0.866	0.834	0.817	0.768	0.731	0.693	0.654	0.615
τ, ns	0.89	0.87	0.85	0.82	0.79	0.78	0.74	0.71	0.68	0.65	0.61
$k_{rad}\cdot10^8$	1.06	1.06	1.06	1.06	1.05	1.05	1.04	1.03	1.02	1.01	1.00
$k_{nrad}\cdot10^8$	10.1	10.4	10.8	11.1	11.6	11.8	12.5	13.1	13.8	14.5	15.3
	C_2H_5OH										
η, cP	1.200	1.096	1.003	0.919	0.834	0.768	0.702	0.647	0.592	0.529	0.483
φ	0.974	0.961	0.939	0.923	0.906	0.883	0.861	0.836	0.814	0.790	0.766
τ, ns	0.84	0.78	0.76	0.75	0.74	0.72	0.71	0.69	0.67	0.66	0.64
$k_{rad}\cdot10^8$	1.16	1.24	1.24	1.23	1.23	1.22	1.22	1.21	1.21	1.20	1.19
$k_{nrad}\cdot10^8$	10.7	11.6	11.9	12.1	12.3	12.6	13.0	13.3	13.6	14.0	14.4

η dynamic viscosity of the solvent, φ luorescence quantum yield, τ excited state molecule lifetime, $k_{rad}\bullet10^8$ radiative deactivation rate constant, $k_{nrad}\bullet10^8$ non-radiative deactivation rate constant

The increase of the viscosity is accompanied by the clearly pronounced growth of the fluorescence intensity and the minor increase of the absorption of the solution (Fig. 3).

The more detailed analysis of photophysical characteristics changings under the viscosity variation is demonstrated below (Table 3). The increase of relative quantum yield and the decrease of the excited state lifetime were observed for all investigated dye-solvent systems. The average fluorescence quantum yield change is~0.25, this let us classify the studied compounds as intensive fluorescent molecular rotors. High Forster-Hoffman constant *X* values (in some cases even higher than the same values for other commercially available fluorescent molecular rotors [24, 25]) are in agreement with this statement.

The types of the photophysical characteristics changes of all studied systems are the same (Fig. 4) – the growth of the viscosity leads to dramatically decrease of non-radiative deactivation constants, the increase of excited state lifetime, while radiative deactivation constants stay practically the same. Such dependence is typical for true molecular rotors, which fluorescent characteristics depend mainly on the dynamic viscosity of the solvent, but not on its temperature or the nature of solvation interactions.

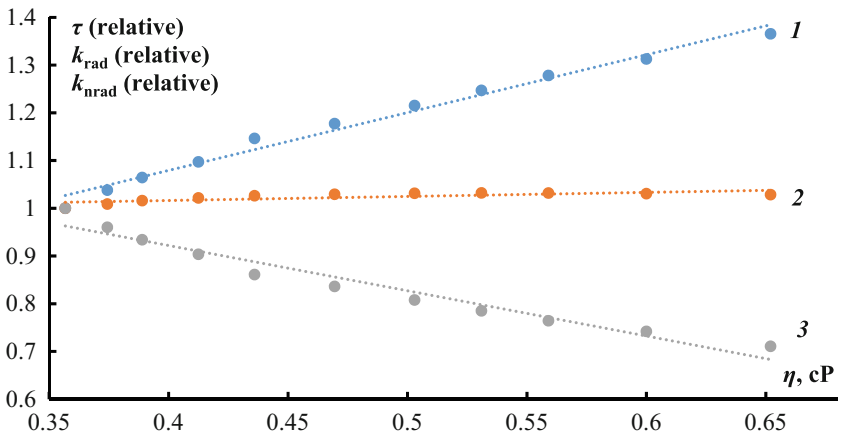

Fig. 4 The change of relative photophysical characteristics of ***3*** with the growth of the dynamic viscosity in C_6H_6: *1* – excited state lifetime (τ), *2* – radiative deactivation rate constant (k_{rad}), *3* – non-radiative deactivation rate constant (k_{nrad})

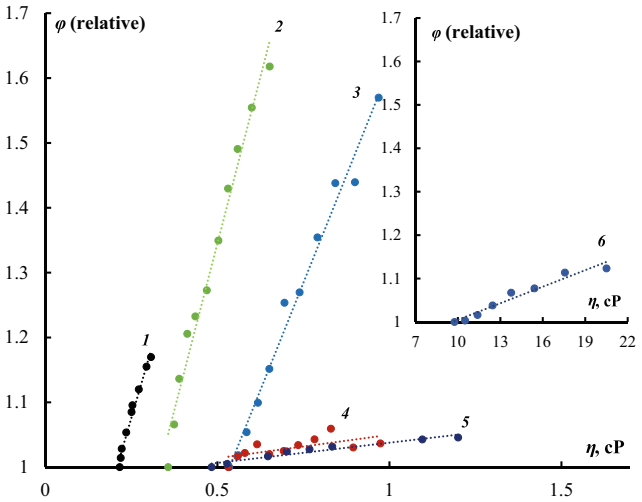

Fig. 5 Change of the relative quantum yield of fluorescence of compound ***2*** in the individual organic solvents: *1* – C_6H_{12}, *2* – C_6H_6, *3* – CCl_4, *4* – C_5H_5N, *5* – C_2H_5OH, *6* – $CH_3CH(OH)CH_3$

The information about spectral characteristics of the compound ***1*** and its analogues can be found in literature as well as compounds with no alkyl substituents at the 1,7-positions [26–28]. Although, the presence of methyl substituents in the dipyrrin core impedes the rotation of bulky substituent, but as shown by the authors of aforementioned publications, the partial overlapping of dipyrrin and phenyl substituent electronic systems could lead to a change in the cross section of the potential energy in the excited state in the case of methylated compounds. So the methylated compounds could be considered as molecular rotors, this fact was confirmed by the intense change of fluorescence under the viscosity variations.

The Influence of the Solvent Nature on Photophysical and Molecular Rotor Properties

The influence of the nature of the solvent on the photophysical properties of compounds was studied on the example of the compound ***2***. The strongest fluorescent molecular rotor properties were observed in nonpolar solvents – benzene, carbon tetrachloride, cyclohexane (Fig. 5). The increase of solvent polarity (by using ethanol, 2-propanol, pyridine, or their mixtures) leads to decrease of the relative quantum yield and its change under the solvent viscosity variation. The decrease of rotary properties in proton donor alcohols and electron donor pyridine is equal, indicating equal influence of universal interactions and specific solvation. The information about decrease of fluorescence intensity in media with high polarity could be found in the literature [28]. This effect was explained by the growth of polarity in the excited molecule exited state, increasing the ability of nonradiative deactivation. This is confirmed by high values of corresponding rate constants and short lifetimes of the excited state in ethanol (see Table 2). The presence of donor nitrogen atom in the 8-substituent should be also taken into account due to its ability for protonation under acidic conditions. The information about pH sensing ability of the BODIPY with the same 8-substituent could be found in literature [6, 29, 30]. The increase of polarity leads to drastic decrease of Forster-Hoffmann constant for ***2***, making this compound ineffective as fluorescent molecular rotor in polar media. Lesser decrease of Forster-Hoffman constants was observed for ***1*** and ***3***. The decrease of molecular rotor properties of BODIPYs in polar media was found by the authors for the first time in literature.

The ability of compound ***2*** to reversibly attach proton could be used to for fluorescent pH indication. This phenomenon was being studied by the titration of the solution of ***2*** in water-ethanol mixture with aqueous hydrochloric acid (c_{HCl}=2 M) (Fig. 6).

With the increase of acidity the bathochromic shift in the absorption and fluorescence spectra was observed, as well as a significant increase in fluorescence intensity. The fluorescence

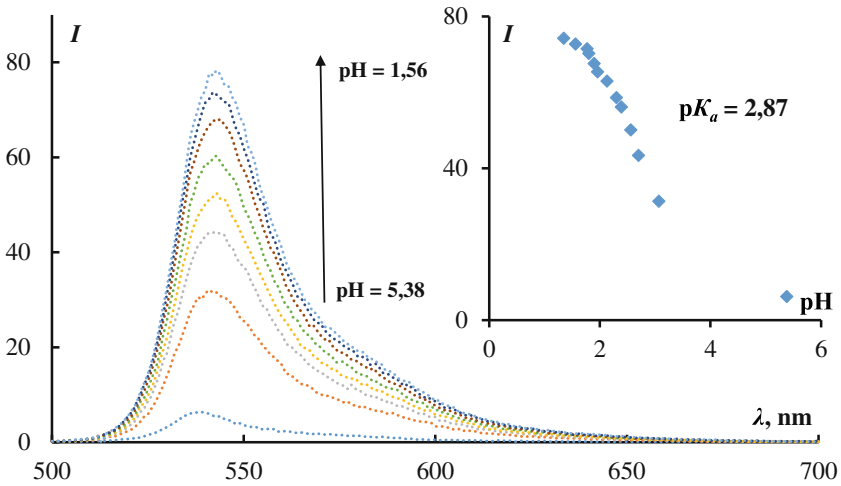

Fig. 6 Fluorescence spectra of ***2*** solution and fluorescence maxima intensity (incut) in water – ethanol mixture ($\varphi_{ethanol}$=0.5) under the pH variation

Table 4 Coefficients (a, b, c, d) of the solvent parameters (*SPP* – solvent polarity/polarizability; *SA* – solvent acidity; *SB* – solvent basicity; η – solvent dynamical viscosity), reliability of approximation (R^2)

		$a(SPP)$	$b(SA)$	$c(SB)$	$d(\eta)$	R^2
Regression with the use of Catalan parameters	φ	1.399	0.174	−1.237	–	0.791
	λ_{abs}	20.128	−9.843	−7.742	–	0.399
	λ_{fl}	21.520	−8.973	−4.847	–	0.937
	$\Delta\lambda$	1.391	0.871	2.894	–	0.154
Regression with the use of Catalan parameters and normalized dynamic viscosity	φ	−1.705	−0.854	0.894	−0.719	0.990
	λ_{abs}	−57.605	−35.597	45.637	−18.002	0.973
	λ_{fl}	19.203	−9.740	−3.257	−0.5365	0.939
	$\Delta\lambda$	76.808	25.857	−48.893	17.466	0.880

intensity increased 12-fold than the original, the unprotonated form. The calculated value of pK_a was 2.87, what's consistent with the data on the acidity constants of alkyl amines, as well as previously studied BODIPY. The change of fluorescence is reversible, after addition of alkali to the solution the drop of fluorescence to the original value was observed.

The contribution of different solvent parameters has been studied by the method of linear regression. The Catalan solvent parameters set - *SPP*, *SB*, *SA*, characterizing the contribution of polarity, acid and basic properties of the solvent, has been used [31, 32]. Traditional approach of the solvatochromic effects description shows low efficiency (Table 4). The received regression coefficients are low and the obtained model does not allow interpreting the experimental results. This model does not reflect the negative solvatochromic effect and fluorescence quenching in polar solvents. Same results were obtained by Chaudhuri et al. for the 8-phenyl substituted analogue of commercially available 4,4-difluoro-8-methyl-1,3,5,7-tetramethyl-2,6-diethyl-4-boron-3a,4a-diaza-s-indacene (PM567, [33]). The obtained low correlation coefficients could be described by the low solvatochromic response of the compound. But we can assume that the bulky substituent in the 8-position could be. Thereby, the authors used dynamic viscosity as the additional parameter (the viscosity parameter was normalized by the most viscous of the used solvent – 2-propanol). In this case we obtained the significant increasing of approximation reliability. The negative coefficients of *SPP* parameter confirm the experimental data. Nonetheless, the obtained coefficients of the viscosity parameter were lower than they were expected. So the analysis of photophysical characteristics changing should mention both polarity of the solvent, its ability to interact with the solute and the dynamical viscosity of the system. The photophysical properties extrapolation in dependence of the viscosity is possible only within the homologous series of solvents [34].

Table 5 Values of Forster-Hoffman equation constant X for different solvents

Solvent	Viscosity range $\eta_{293} - \eta_{343}$	X
C_6H_6	0.357–0.652	0.5949
CCl_4	0.534–0.969	0.8379
C_6H_{12}	0.615–0.951	1.1534
C_2H_5OH	0.483–1.200	0.5354
C_3H_7OH	11.5–17.7	0.3662
C_3H_7OH – $C_3H_5(OH)_3$ $\chi_{glycerol}$=0.3	46–110	0.1193
C_3H_7OH – $C_3H_5(OH)_3$ $\chi_{glycerol}$=0.5	128–353	0.0974
C_3H_7OH – $C_3H_5(OH)_3$ $\chi_{glycerol}$=0.7	400–1444	0.086

The molecular rotors properties in high viscosity range were studied on the example of the compound ***1***. The changing of fluorescent characteristics was monitored in the viscosities range of 11.5 up to 1444 cP by using 2-propanol – glycerol mixtures with different molar ratios of the components. The dependence of the fluorescence intensity on the dynamic viscosity of the solution maintained at the all entire range of viscosities. At the same time, the decrease of the inclination angle of the relative quantum yield plot and the decreasing of the X constant in the Forster-Hoffman equation indicates that the growth of the mole fraction of the glycerol leads to a decrease of rotary properties of investigated compounds (Fig. 6).

Molecular rotor characteristics also weaken in low-viscous media. The highest value of constant X (the indicator of the rotary properties manifestation) for the compound ***1*** was obtained in cyclohexane (Table 5 and Fig. 7), the values of constant X in less viscous solvents – benzene and CCl_4 – were smaller.

Thus, it can be stated that every fluorophore has its own optimal viscosity range (Fig. 8), where its rotary properties are the most intensive. The position and width of this range depends on both nature of the fluorophore (the nature of the

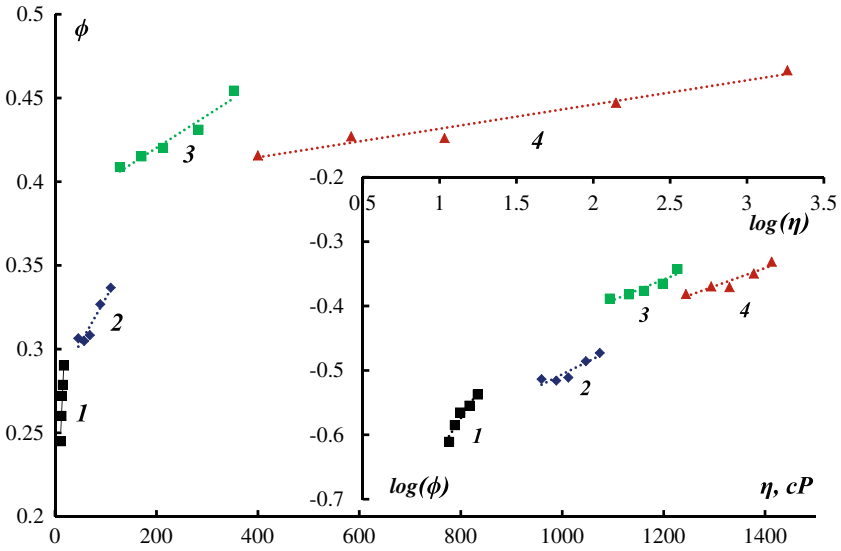

Fig. 7 The dependence of the fluorescence quantum yield on the dynamic viscosity of the binary (2-propanol – glycerol) solvent: *1* – $\chi_{glycerol}$=0; 2 – $\chi_{glycerol}$=0.3; *3* – $\chi_{glycerol}$=0.5; *4* – $\chi_{glycerol}$=0.7

bulky substituent, the value of the energy barrier of the transition to the TICT state) and on the nature of the solvent media (the ability to specific solvation, chemical interaction with the solute).

Conclusions

Several BODIPY-based fluorescent dyes were synthesized and characterized. The photophysical properties of these dyes have been systematically investigated in different solvents and solvent mixtures. Synthesized compounds could be used as perspective viscosity and polarity sensors in different systems. Minor changes in the nature of the substituent in the 8- position does not influence the spectral properties, but the presence of nitrogen donor atom in case of compound ***2*** could be used for the sensing of the donor-acceptor interactions with solvent or dissolved compounds. The new approach of spectral properties correlation with solvent parameters was proposed, and the viscosity parameter should be taken into account in case of BODIPYs with the bulky substituents. The intensity of fluorescence molecular rotor properties of investigated compounds depend on the viscosity range of the media and for the investigated compounds decrease gradually with the viscosity increase above 1 cP.

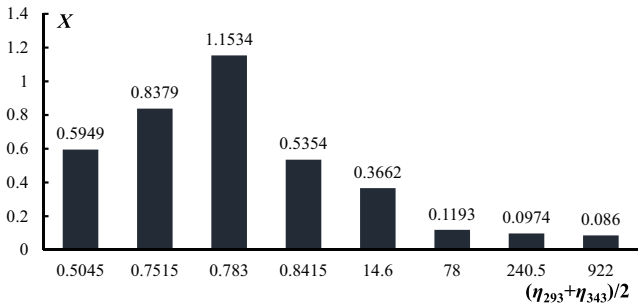

Fig. 8 Values of Forster-Hoffman equation constant *X* in dependence on the values of the viscosity range middle for the current solvent ($(\eta_{293}+\eta_{343})/2$)

Acknowledgments The work was supported by the grants of the Russian Foundation for Basic Research (No 14-03-31888, No 15-33-20002) and the grant of the President of the Russian Federation for young scientists and graduate students engaged in advanced research and development in priority directions of modernization of the Russian economics (2013 – 2015) (Grant No. SP-1742.2013.1).

References

1. Wang LY, Fang GP, Cao DR (2015) A novel phenol-based BODIPY chemosensor for selective detection Fe3+ with colorimetric and fluorometric dual-mode. Sensors Actuators B Chem 207: 849–857
2. He Y, Feng RK, Yi YR, Liu ZX (2014) Recent progress in the research of borondipyrromethene-based fluorescent ion chemosensor. Chinese J Org Chem 34:2236–2248
3. Madhu S, Kalaiyarasi R, Basu SK, Jadhavb S, Ravikanth M (2014) A boron-dipyrrin–mercury (II) complex as a fluorescence turn-on sensor for chloride and applications towards logic gates. J Mater Chem C 2:2534–2544
4. Liu J, He XX, Zhang J, He T, Huang LQ, Shen JQ, Li D, Qiu HY, Yin SC (2015) A BODIPY derivative for colorimetric and fluorometric sensing of fluoride ion and its logic gates behavior. Sensors Actuators B Chem 208:538–545
5. Gareis T, Huber C, Wolfbeis OS, Daub J (1997) Phenol/phenolate-dependent on/off switching of the luminescence of 4,4-difluoro-4-Bora-3a,4a-diaza-S-indacenes. Chem Commun 18:1717–1718
6. Werner T, Huber C, Heinl S, Kollmannsberger M, Daub J, Wolfbeis OS (1997) Novel optical Ph-sensor based on a boradiaza-indacene derivative. Fresenius J Anal Chem 359:150–154
7. Sui B, Tang S, Liu T (2014) Novel BODIPY-based fluorescence turn-on sensor for Fe^{3+} and its bioimaging application in living cells. ACS Appl Mater Interfaces 21:18408–18412
8. Andrea B, Costero M, Salvador AG (2014) Chromo-fluorogenic BODIPY-complexes for selective detection of V-type nerve agent surrogates. Chem Commun 50:13289–13291

9. Fengling S, Yingying X, Xu W, Jingyun W, Xiaoqing X, Xiaojun P (2014) Ratiometric fluorescent probe based on novel red-emission BODIPY for determination of bovine serum albumin. Chem Res Chin Univ 30:738–742
10. Ma D, Kim D, Seo E, Lee S, Ahn KH (2015) Ratiometric fluorescence detection of cysteine and homocysteine with a BODIPY dye by mimicking the native chemical ligation. Analyst 140:422–427
11. Bahaidarah E, Harriman A, Stachelek P, Rihn S, Heyerb E, Ziessel R (2014) Fluorescent molecular rotors based on the BODIPY motif: effect of remote substituents. Photochem Photobiol Sci 10:1397–1401
12. Marfin YS, Merkushev DA, Levshanov GA, Rumyantsev EV (2014) Fluorescent properties of 8-phenylBODIPY in ethanol – ethylene glycol mixed solutions. J Fluoresc 24:1613–1619
13. Rongrong H, Lager E, Aguilar-Aguilar A, Liu J, Lam JWY, Sung HHY, Williams ID (2009) Twisted intramolecular charge transfer and aggregation-induced emission of BODIPY derivatives. J Phys Chem C 113:15845–15853
14. Dal Molin M, Verolet Q, Soleimanpour S, Matile S (2015) Mechanosensitive membrane probes. Chemistry 21:6012–6021
15. Haidekker M, Theodorakis E (2010) Environment-sensitive behavior of fluorescent molecular rotors. J Biol Eng 4:11–25
16. Benniston AC (2014) Monitoring rheological properties in biological systems by fluorescence spectroscopy using borondipyrromethene (Bodipy) dyes: a mini review. J Anal Bioanal Tech 5:1–11
17. Forster T, Hoffmann G (1971) Effect of viscosity on the fluorescence quantum yield of some dye systems. Z Phys Chem 75:63–76 **(in German)**
18. Weissberger A, Proskauer ES, Riddick JA, Toops EE (1955) Organic solvents. Physical properties and methods of purification. Interscience Publishers Inc, New York
19. Bruttel P, Schlink R (2003) Water determination by Karl Fischer titration. Metrohm Monogr 8(5003):2003–2009.
20. Wolfbeis OS (2008) Standardization and quality assurance in fluorescence measurements techniques. Springer Ser Fluoresc. doi:10.1007/978-3-540-75207-3
21. Marfin YS, Rumyantsev EV, Ya SF, Antina EV (2012) Relationship between the spectral properties of solutions of borofluoride complex of alkylated dipyrromethene and the physicochemical parameters of solvents. Russ J Phys Chem A 86:1068–1072
22. Arbeloa TL (1999) Correlations between photophysics and lasing properties of dipyrromethene–bf_2 dyes in solution. Chem Phys Lett 299:315–321
23. Volchkov VV, Khimich MN, Ya MM, Uzhinov BM (2013) A fluorescence study of the excited-state dynamics of boron dipyrrin molecular rotors. High Energy Chem 47:224–229
24. Jeyanthy S, Lichlyter D, Wright NE, Dakanali M, Haidekker M, Theodorakis E (2010) Molecular rotors: synthesis and evaluation as viscosity sensors. Tetrahedron 66:2582–2588
25. Giulio M, Martinelli E, Ruggeri G, Galli G, Pucci A (2015) Julolidine fluorescent molecular rotors as vapour sensing probes in polystyrene films. Dye Pigment 113:47–54
26. Ling KH, Kirmaier C, Yu L, Thamyongkit P, Youngblood WJ, Calder ME, Ramos L et al (2005) Structural control of the photodynamics of boron - dipyrrin complexes. J Phys Chem B 109: 20433–20443
27. Gordon H, Ruseckas A, Harriman A, Samuel IDW (2011) Conformational effects on the dynamics of internal conversion in boron dipyrromethene dyes in solution. Angew Chem Int Ed 50: 6634–6637
28. Rezende LC, Vaidergorn M, Moraes JCB, da Silva Emery F (2014) Synthesis, photophysical properties and solvatochromism of meso-substituted tetramethyl BODIPY dyes. J Fluoresc 24:257–266
29. Banuelos J, Lopez Arbeloa F, Arbeloa T, Salleres S, Vilas JL, Amat-Guerri F, Liras M, Lopez Arbeloa I (2008) Photophysical characterization of new 3-amino and 3-acetamido BODIPY dyes with solvent sensitive properties. J Fluoresc 18:899–907
30. Lager E, Liu J, Aguilar-Aguilar A, Zhong Tang B, Pena-Cabrera E (2009) Novel meso-polyarylamine-BODIPY hybrids: synthesis and study of their optical properties. J Org Chem 74:2053–2058
31. Banuelos PJ, Lopez Arbeloa F, Martinez Martinez V, Lopez Arbeloa T, Lopez Arbeloa I (2004) Photophysical properties of the pyrromethene 597 dye: solvent effect. J Phys Chem A 108: 5503–5508
32. Marfin YS, Rumyantsev EV (2014) Analysis of solvation and structural contributions in spectral characteristics of dipyrrin Zn(II) complexes. Spectrochim Acta A Mol Biomol Spectrosc 130:423–428
33. Chaudhuri T (2010) Photophysical properties of the 8-phenyl analogue of PM567: a theoretical rationalization. Spectrochim Acta A Mol Biomol Spectrosc 75:739–744
34. Alamiry MAH, Benniston AC, Copley G, Elliott KJ, Harriman A, Stewart B, Zhi YG (2008) A molecular rotor based on an unhindered boron dipyrromethene (Bodipy) dye. Chem Mater 20:4024–4032
35. Krestov GA, Afanas'yev VN, Yefremova LS (1988) Physical and chemical properties of binary solvents: handbook. Khimiya, Leningrad, p 688. (in Russian)